Journal of Ultrafine Grained and Nanostructured Materials
https://jufgnsm.ut.ac.ir
Vol. 55, No.1, June 2022, pp. 58-64
Print ISSN: 2423-6845 Online ISSN: 2423-6837
DOI: 10.22059/jufgnsm.2022.01.09

Investigation of mechanical and EMI shielding performance of polypropylene (PP)/carbon nanotube (CNT)/glass fiber microcellular foam

Mahdi Gholampour*[*,1,2], Mohammad Aghvami-Panah[3], Seyed Reza Ghaffarian Anbaran*[*,3]

[1]Physics and Chemistry Group, Faculty of basic sciences, Imam Ali University, Tehran, Iran;
[2]Nanomaterials Group, Department of Materials Engineering, Tarbiat Modares University, Tehran, Iran;
[3]Department of Polymer Engineering & Color Technology, AmirKabir University of Technology, Tehran, Iran.

Recieved: 14 October 2021; Accepted: 8 January 2022

**Corresponding author email: Mahdi.gholampour@modares.ac.ir, Sr_ghaffarian@aut.ac.ir*

ABSTRACT

Polypropylene (PP)/Carbon-Nanotube (CNT) nanocomposites and PP/CNT/Glass fiber (GF) hybrids were foamed using supercritical carbon dioxide (CO_2) through a batch foaming process. Uniform nanofiller dispersion was assessed by field emission scanning electron microscopy (FE-SEM). By incorporating CNTs in the matrix, the average cell size was reduced to less than one-second that of neat foam (from 49 to 22.5 µm), and cell density increased. As a matter of fact, high electrical conductivity is crucial to achieving a great electromagnetic interference (EMI) shielding performance. Hence, CNTs were loaded up to 3 wt%. By incorporation of CNTs, electrical conductivity increased from ~10^{-16} to ~10^{-4} and ~10^{-5} S/cm for unfoamed and foamed PP/CNT3 samples, respectively, and EMI shielding effectiveness increased to 11 dB and 9.5 dB for unfoamed and foamed PP/CNT3 samples, respectively. After evaluating the microstructural and electrical properties of the nanocomposites and their foams, as well as elucidating the foaming process's role in the EMI shielding performance of the hybrids and foams, there was a great need to investigate the mechanical properties of hybrid systems and the effect of fiber concentration. Tensile properties revealed that by increasing the fiber content, young modulus and tensile strength increased for unfoamed samples and decreased for foams. The compression test of hybrid foams showed that by loading nanotubes and glass fibers, compressive mechanical properties increased. Also, by adding CNTs and glass fibers, impact properties increased and decreased, respectively, for solid and foamed hybrids. Moreover, by loading both additives impact properties enhanced.

Keywords: *Microcellular Foam; Nanocomposite; Hybrid; EMI shielding; Mechanical Properties.*

1. Introduction

In the last decade, nanocomposite foams have attracted a great deal of interest in numerous research fields due to their superior strength-to-density ratio, impact, electrical, and thermal properties [1,2]. Recently, polymeric composite foams containing carbonaceous fillers have attracted electromagnetic interference (EMI) shielding applications [3,4]graphene nano-ribbon (GNR. As electronic devices and communication instruments are being fully-fledged, it is expected to be crucial to reduce electromagnetic pollutions. Compared to the metal-based EMI shielding materials, carbonaceous polymer composites and their foams have some advantages, including lightweight, easy processing, and broad absorption bandwidth [5,6]. Light weighting of the EMI shielding materials has been applied through various procedures. One of the practical methods to achieve this purpose is Solid-state batch foaming [5,7–9]. As a matter of

fact, micro and nano-sized fillers could ameliorate and enhance electrical conductivity and shielding features of polymer foams in which these properties depend on filler size, shape, concentration, and aspect ratios [8]. Yang et al. prepared polystyrene (PS)/carbon nanofiller composite foams using a chemical blowing agent. They found that the EMI shielding effectiveness (SE) of the as-produced composite foams were 14 dB for 10 wt % nanofiber loading and 19 dB for 15 wt % nanofiber loading, respectively [10]. Moreover, Zhang et al. fabricated PMMA/graphene foams using supercritical CO_2 with 5 wt % graphene loading exhibited an EMI SE of 13–19 dB [11]. Other polymer systems such as polyurethane (PU)[12] and polyethylene (PE) [13]} problems with electromagnetic interference (EMI have also been used for the fabrication of EMI shielding microcellular foams materials. However, scant attention has been attracted to the simultaneous improvement of shielding properties and mechanical performances.

The electrical conductivity potentially endows lightweight nanocomposite foams with good electromagnetic interference (EMI) shielding property. In this study, the overall EMI SE was calculated based on the S-parameters as follows [8]:

$$\text{EMI SE} = \text{SE}_\text{A} + \text{SE}_\text{R} + \text{SE}_\text{M} = 10\log\frac{1}{|S_{21}|^2} = 10\log\frac{1}{|S_{12}|^2}$$

Where $|S_{ij}|^2$ represents the power transmitted from port i to port j. The total EMI shielding (SE_T) includes the shielding by absorption (SE_A) and the reflection (SE_R), and SE_M, which is the microwave multiple internal reflections and could be negligible when the thickness of the foamed material is more than the skin depth, especially in composite foams containing conductive fillers, because most reflected radiation inside the material is absorbed [8]. In the reflection mechanism, surface free charges are responsible for reflecting the incoming waves from the surface of the material, which is attributed to the difference between the impedance of incoming waves and the shielding material. Thus, high electrical conductivity can increase the reflection mechanism. The materials that can attenuate wave energy into thermal energy are capable of the absorption mechanism. In addition, dielectric and magnetic loss have dominant roles in the absorption mechanism. The multiple reflection mechanism is related to radiation scattering within a material because of the material's inhomogeneity [14–16].

Some restrictions such as poor tensile strength, poor surface quality, and low thermal and dimensional stability for polymeric foams limited their engineering usage. Fibers can act as the most potential enhancer, and there is now a substantial body of literature that investigated their influence on foams. The presence of fibers in the polymeric foams can adjust the final properties; indeed, fibers not only significantly increase tensile and compression modulus as well as strength but also can control the nucleation and growth rate of cells. Glass fiber (GF) is one of the most commonly used fibers for enhancing the mechanical properties of polymers due to its low density, high tensile strength, high chemical resistance, and low price [17,18]. Aghvami-Panah et al. investigated the impact of ultra-high molecular weight polyethylene fiber on mechanical properties of LDPE/MWCNT microcellular foams. They introduced that by only 15 wt.% tensile properties significantly enhanced [19]. However, they used unidirectional fibers that improve tensile properties substantially in one direction. So, it was necessary to conduct a research on improving mechanical properties in 3D-direction.

The current study aims to take advantage of simultaneous benefits of the GF and CNT incorporation in both EMI shielding performance and mechanical properties improvement. To do so, there is a great need to investigate the microstructural properties; hence, the effect of microcellular foaming and weight fraction of the components on the solids and foams were examined.

2. Experimental details

2.1. Materials

RPX-120L grade of PP (MFI: 6 g/10 min) with a density of 0.92 g/cm^3 was purchased from Jam Petrochemical Co. CNTs were supplied by Nanocyl™, Belgium. CNTs were multi-walled and produced by Catalytic Carbon Vapor Deposition (CVD) with an average outer diameter of 10 nm, an average length of 1.5 μm, a surface area of 250-300 m^2/g, carbon purity of 90%, and a density of 1.44 g/cm^3. Taiwan glass 203P grade Glass fibers with an average length of 3mm and 13μm diameter and a density of 2.44 g/cm^3 were used in this study as the reinforcement.

2.2. Methods

The PP/MWCNT/GF hybrids were prepared by melt compounding in a Brabender (Plasticorder

W50) with a temperature of 200 °C, rotor speed of 80 rpm, and a mixing time of 10 min. Subsequently, samples were compression molded at 180 °C and 50 MPa for 5 min.

A batch foaming process via supercritical CO_2 was used to produce cellular structure in the nanocomposites and the hybrids. Samples were first placed in an autoclave vessel containing a syringe pump. Then, the autoclave was fed by a CO_2 capsule to reach the saturation pressure of 170 bar. After the saturation time (60 min), foams were produced through a fast pressure drop at 134 °C.

2.3. Characteristics

Scanning electron microscopy (SEM) (SERON AIS-2100) was applied to discover the dispersion and distribution of carbon nanotubes in the PP matrix and the cell morphology of the foams. The samples were broken in liquid nitrogen, and then the fractured surface was coated with gold. The image processing software, ImageJ, was used to measure the cell density and the average cell size. The densities of the composites and foams were measured via the water displacement method in accord with ASTM D792. Expansion ratio and porosity were calculated trough ρ_s/ρ_f, 1-(ρ_f/ρ_s), respectively. Cell density was calculated by the following equation [20]:

$$N = \left(\frac{n}{A}\right)^{3/2} \times \frac{\rho_P}{\rho_F} \quad (2)$$

Where n is the number of cells in the A area of the micrograph. The DC volume electrical conductivity of the samples was measured with a 4-probes KEITHLEY 610C electrometer (KEITHLEY Instruments Inc., Cleveland, Ohio). The sample surfaces were coated with gold to reduce the contact resistance between the electrodes and the sample. Three samples were tested for each composite and foam, and the average value was reported as a final result.

A vector network analyzer, Hewlett Packard 8410C (USA), was used to measure EMI SE over the frequency range of 8.2– 12.4 GHz (X-band). The samples were cut into rectangle plates with a dimension of 22 × 11 mm^2 to fit the waveguide sample holder. The thickness of the samples was about 2.5 mm. Also, foamed ones were carefully cut to reach the same dimension. The tensile properties were measured on a GALDABINI Sun2500 mechanical testing machine at room temperature. Foam samples were used for tensile testing with a thickness ranging from 3 to 4 mm, depending on the samples' expansion ratio. Four specimens were tested at 50 mm⁄min for each composition, and mean values were reported. Also, the uniaxial compression test with a 1mm/min displacement rate was performed to characterize the compressive properties of the PP/CNT/GF composite foams.

3. Results and discussion

SEM micrographs were assessed to detect the dispersion and morphology of the nanotubes and fibers in the PP matrix. As presented in Figure 1a, single CNTs, or small bundles of them, are uniformly dispersed and distributed throughout the matrix. Also, It could be seen that glass fibers were randomly allocated into the PP matrix.

Figure 2 shows illustrative SEM micrographs of the cross-sectioned nanocomposite and hybrid foams with various carbon nanotube and GF contents. It is evident that average cell size decreased with an increase in nanotube content. However, the foam density and cell density were enhanced. The

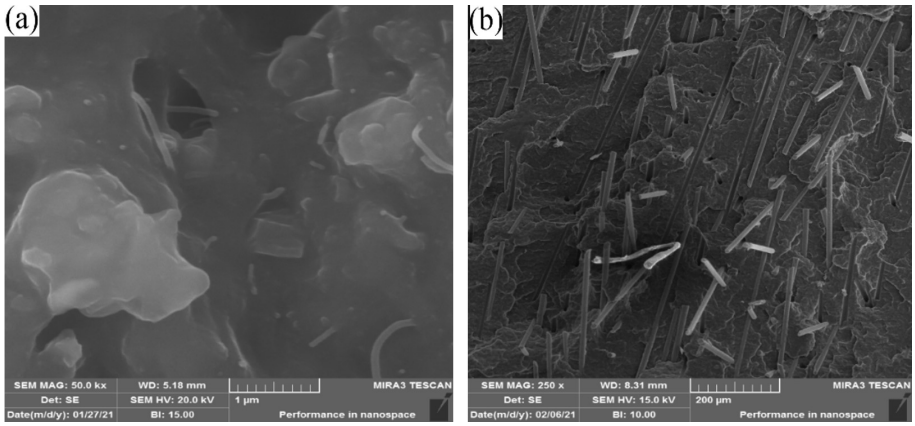

Fig. 1- FE-SEM images of cryo-fractured surfaces of PP/CNT3 and PP/CNT3/GF10.

cellular structure improvement by incorporating CNTs could be attributed to enhancing foaming heterogeneous cell nucleation via loading the nanotubes, which increase nucleation sites [19]. It is worthy of mention that the presence of nanotubes could itself improve melt strength, which could be considered as another reason for the improvement in cellular structure. The enhancement in melt strength could prevent gas escape from the cells while avoiding cell coalescence. In the presence of GF, the average cell size increased, and the cell density first decreased and then increased by enhancing the fiber content compared to the nanocomposite foams without glass fiber. It is noteworthy that the larger cells were formed around the fibers, and the number of these large cells increased as the amount of fibers increases. Also, the cells adjacent to these large cells have been significantly reduced. To sum up, these alterations in cellular characteristics could be attributed to; (I) boosting the number of heterogeneous nucleation sites, (II) reduction in gas portion required for the growth of the smaller cells due to the absorbing a great deal of blowing agent into the matrix-fiber interface, and (III) coalescence prevention owing to the increment of melt strength. To better clarify, foam characteristics of all foamed samples are presented in Table 1.

Electrical conductivity is critical for EMI shielding efficiency because it is an intrinsic ability of materials for absorbing electromagnetic radiation [21]. Volume DC electrical conductivity of solid composites as a function of filler content as well as the influence of microcellular cell structure on the electrical conductivity of nanocomposites was investigated, and the results are shown in figure 3a. It is obvious that by the incorporation of CNTs in both solid and foamed samples, the electrical conductivity (EC) increased. For instance, EC of solid and foamed PP/CNT enhanced from ~ 1.6 $\times 10^{-16}$ S/cm and 2.7 $\times 10^{-18}$ S/cm for neat samples to 4.7$\times 10^{-4}$ S/cm and 3.3 $\times 10^{-5}$ S/cm by loading

Table 1- Characteristics of the foams

Sample	Average cell size (μm)	Foam density (g/cm^3)	Unfoamed sample's density (g/cm^3)	Cell density ($cell/cm^3$)	Expansion ratio
PPneat	49	0.068	0.92	7.94×10^7	13.5
PP/CNT1	32.2	0.077	0.92	1.78×10^8	11.9
PP/CNT3	22.5	0.094	0.92	4.86×10^8	9.8
PP/CNT3/GF5	39.9	0.081	0.93	2.27×10^8	11.5
PP/CNT3/GF10	25.4	0.088	0.93	1.78×10^9	10.5
PP/CNT3/GF20	31.4	0.106	0.95	5.83×10^8	8.9

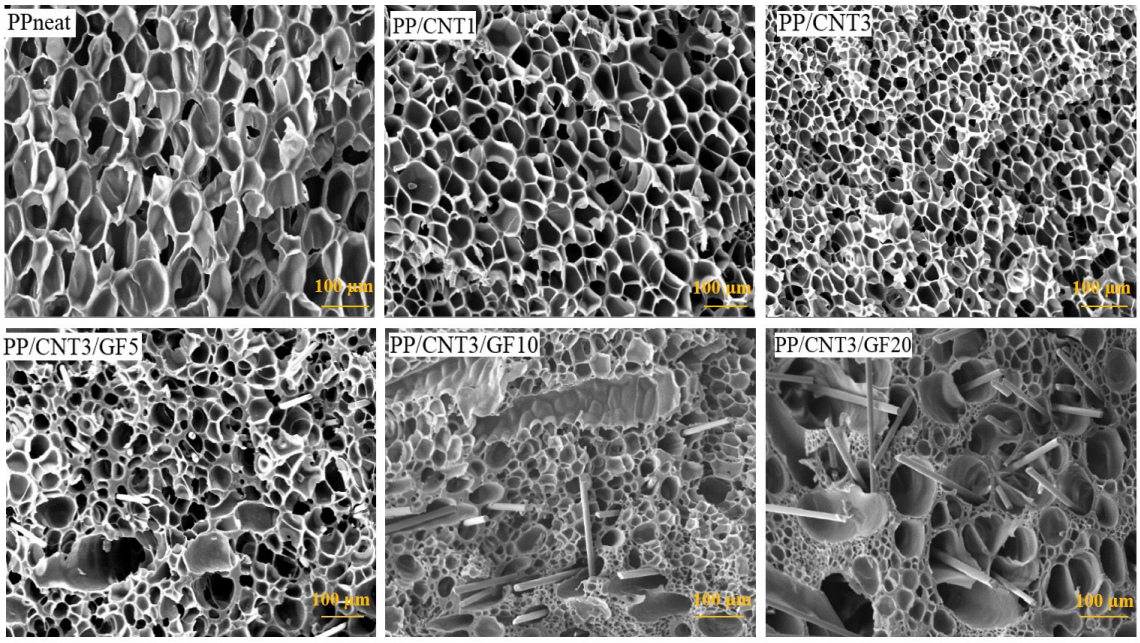

Fig. 2- SEM micrographs and cell size distribution of the produced foams.

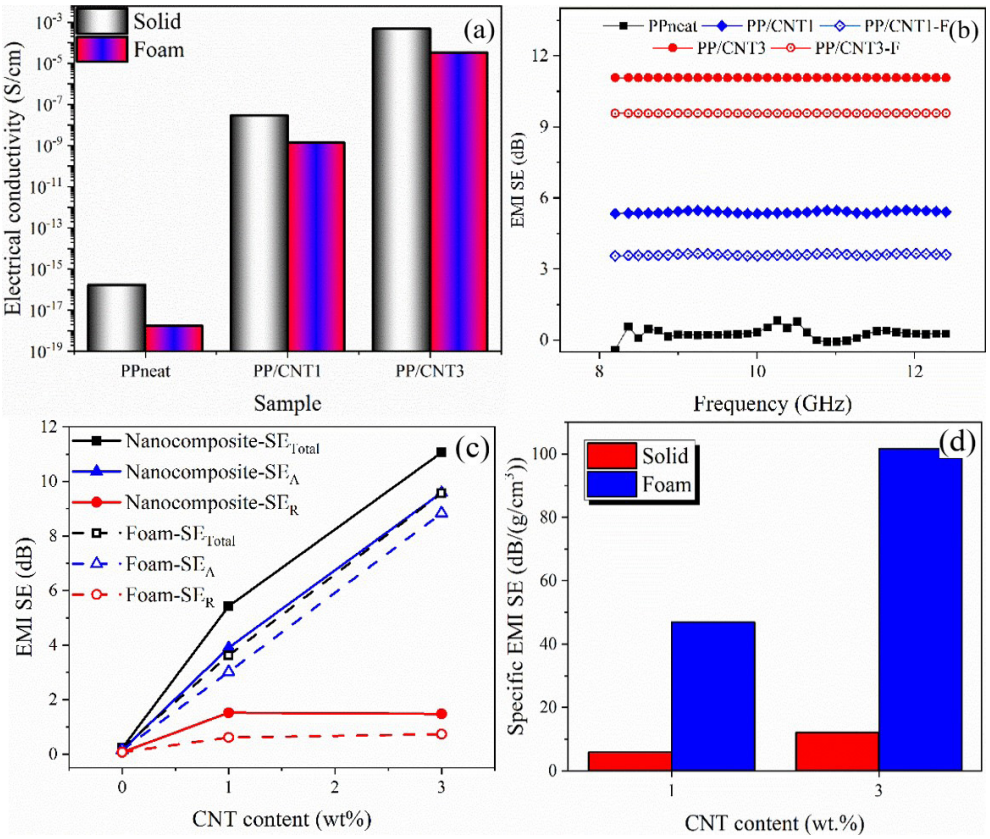

Fig. 3- (a) Electrical conductivity (b) EMI shielding efficiency (c) SETotal, SER, and SEA of nanocomposites and foams (d) Specific EMI shielding efficiency.

CNTs up to 3 wt.%, respectively. Enhancement of the EC by increasing the number of nanotubes can be attributed to increasing the contact surface of carbon nanoparticles, thus establishing the path of movement and facilitating the movement of electrons from one place to another. However, conductivity decreased after introducing the cellular structure. This result stems from the supposition that porous structures can act as obstacles for electron travel and increase the distance of adjacent nanoparticles [22].

The EMI shielding of nanocomposites and their microcellular foams at the X-band (8–12 GHz) were measured and depicted in Figure 3b. Accordingly, we eliminated multiple internal reflections parameter (SE_M) for better examination and comparison study. The results were reported for the solid samples with 2.5 mm thick plates. It is seen from figure 3b that the EMI SE of nanocomposites and microcellular foams exhibited weak frequency dependency at the X-band. The EMI SE of PP/CNT nanocomposites increased up to ~11dB at 3 wt % CNT loading. After the volume expansion by ~10 times, however, the EMI SE of nanocomposite foams decreased. The reason for the difference in EMI SE between the two samples was mainly due to the obvious decrease in electrical conductivity and the actual thickness of microwave radiative transfer in the foamed sample. Therefore, the significant reduction of sample thickness by expansion would inevitably decrease the EMI SE of nanocomposite foam. Figure 3c summarizes the contribution of SE_A and SE_R. The introduction of the microcellular structure was verified to further increase the contribution of SE_A to SE_T, where about 92.2% electromagnetic energy was absorbed by the microcellular foams, suggesting the obvious increased absorbing ability of samples with the presence of microcellular structure.

The specific EMI shielding efficiency was calculated based on the rate of total EMI shielding efficiency and the sample density, and the results are shown in figure 3d. Owing to the much lower density of the foamed hybrids, the specific EMI shielding efficiency, which represents the material utilizing efficient, would be higher than the solid

counterparts. For instance, the specific EMI SE of microcellular PP/CNT3 foams was ~110 dB/(g/cm^3). These results demonstrated that the foaming process dramatically improved the specific EMI SE of PP/CNT nanocomposites.

After evaluating electrical and shielding properties, it was necessary to investigate mechanical properties. For simplifying the comparative study on mechanical properties, the CNT content maintains constant (3 %wt.). The impact of various fiber concentrations on both solid and foams was explored and depicted in figure 4a. The elastic modulus and yield stress increased after the incorporation of the nanoparticles. However, both the ultimate tensile strength and the elongation at break decreased due to filler interaction with the matrix and the effect on the crystalline structure. It should be stated that the changes in mechanical properties might be attributed to the existing strong interaction between nanoparticles and polymeric matrix that leads to immobilizing the chains. It is also observed that by adding fibers to the system, the modulus and yield stress of the hybrids increased, and the elongation at break and toughness of the reinforced nanocomposites decreased. These alterations can be attributed to the load distribution between the matrix and the fibers. Accordingly, more force was endured by the fibers, which increased the modulus and yield stress. However, poor interaction between the matrix and the fibers further reduces the fracture strain and the toughness. All mechanical properties were dropped, as expected, by incorporating a porous structure. Although these are not comparable with solid specimens, the mechanical properties such as elastic modulus and tensile strength of PP/CNT3 increased despite a reduction in foam density, resulting from the increase of nanotube content. Surprisingly, the tensile properties of hybrid foams reduced as fiber's content increased. According to the SEM micrographs of the foams, as the amount of fibers increased, the cells induced around the fibers enlarged. As aforementioned, the size of the cells is inversely proportional to the mechanical properties. Moreover, fibers have an insignificant part in load-bearing since they are located in the center of the cells with loose fiber-matrix interfacial interaction. Hence, the reduction in mechanical properties of foams can be credited by the increase in the number of large cells and loose interaction between PP chains and glass fibers.

The compressive strength of the PP/CNT and PP/CNT/GF nanocomposite foams are presented in Figure 4b. Obviously, the PP/CNT foam showed higher compressive strength than that of the pure one, attributing to the higher cell density, more uniform and smaller cell size of the nanocomposite parts, as well as the enhancement of the well-dispersed MWCNT on the cell walls [23]. Moreover, by increasing the fibres' content, Young's modulus and the collapse stress increased. These improvements in mechanical properties could have resulted from the presence of fibers with much higher strength and modulus, which enhanced the strength of the cell walls. Also, reducing the average cell size by increasing fiber content could be considered another motivation for improving the final compressive properties. Besides the advantages of smaller cells, the larger cells in the bimodal foams reduce the mass density. Consequently, the overall

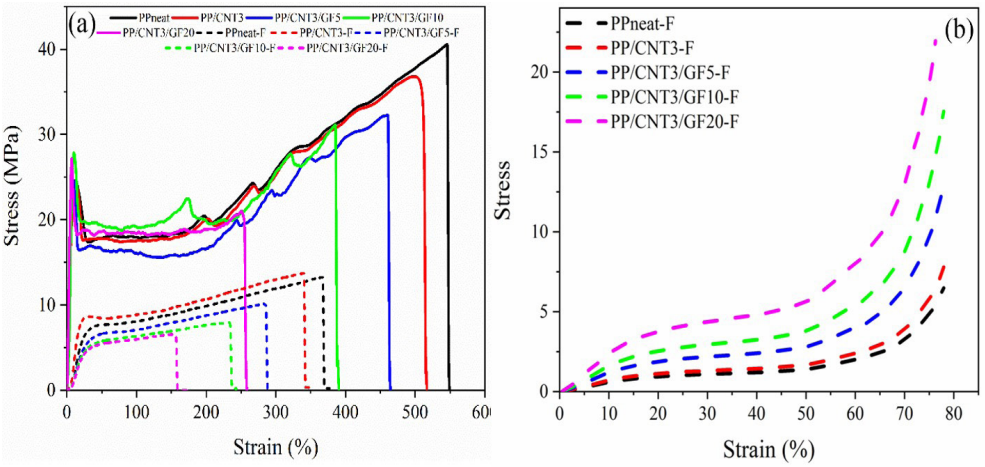

Fig. 4- Stress-strain curves of the samples in (a) tensile and (b) compression mode.

compressive properties are improved dramatically for the bimodal composite foams by maintaining the density reduction.

4. Conclusion

PP/CNT nanocomposites and PP/CNT/GF hybrids were prepared via melt mixing and then foamed through microcellular batch foaming utilizing supercritical CO_2. SEM micrographs depicted that incorporating MWCNTs to the nanocomposite led to decrement and increment of cell size and cell density of microcellular structure, respectively. The electrical conductivity and EMI shielding performance of the nanocomposites and their foams indicated that both EC and EMI SE increased with the addition of nanotubes and diminished by the formation of the cellular structure. Finally, the tensile and compressive properties of the nanocomposites and their foams were investigated. By incorporating both fibers and nanotubes, the modulus and strength for solid samples increased, yet in microcellular foams, the tensile properties reduced as the fiber content enhanced. Hybrids' compressive mechanical properties indicated that Young's modulus and collapse stress increased by loading glass fibers.

References

1. Mohebbi A, Mighri F, Ajji A, Rodrigue D. Current Issues and Challenges in Polypropylene Foaming: A Review. Cellular Polymers. 2015;34(6):299-338.
2. Martínez AB, Realinho V, Antunes M, Maspoch ML, Velasco JI. Microcellular Foaming of Layered Double Hydroxide–Polymer Nanocomposites. Industrial & Engineering Chemistry Research. 2011;50(9):5239-47.
3. Jun Y-s, Habibpour S, Hamidinejad M, Park MG, Ahn W, Yu A, et al. Enhanced electrical and mechanical properties of graphene nano-ribbon/thermoplastic polyurethane composites. Carbon. 2021;174:305-16.
4. Tran M-P, Detrembleur C, Alexandre M, Jerome C, Thomassin J-M. The influence of foam morphology of multi-walled carbon nanotubes/poly(methyl methacrylate) nanocomposites on electrical conductivity. Polymer. 2013;54(13):3261-70.
5. Zhao B, Wang R, Li Y, Ren Y, Li X, Guo X, et al. Dependence of electromagnetic interference shielding ability of conductive polymer composite foams with hydrophobic properties on cellular structure. Journal of Materials Chemistry C. 2020;8(22):7401-10.
6. Che RC, Peng LM, Duan XF, Chen Q, Liang XL. Microwave Absorption Enhancement and Complex Permittivity and Permeability of Fe Encapsulated within Carbon Nanotubes. Advanced Materials. 2004;16(5):401-5.
7. Zakiyan SE, Azizi H, Ghasemi I. Effect of cell morphology on electrical properties and electromagnetic interference shielding of graphene-poly(methyl methacrylate) microcellular foams. Composites Science and Technology. 2018;157:217-27.
8. Panahi-Sarmad M, Noroozi M, Abrisham M, Eghbalinia S, Teimoury F, Bahramian AR, et al. A Comprehensive Review on Carbon-Based Polymer Nanocomposite Foams as Electromagnetic Interference Shields and Piezoresistive Sensors. ACS Applied Electronic Materials. 2020;2(8):2318-50.
9. Aghvami-Panah M, Jamalpour S, Ghaffarian SR. Microwave-assisted foaming of polystyrene filled with carbon black; effect of filler content on foamability. SPE Polymers. 2021;2(1):86-94.
10. Yang Y, Gupta MC, Dudley KL, Lawrence RW. Conductive Carbon Nanofiber-Polymer Foam Structures. Advanced Materials. 2005;17(16):1999-2003.
11. Zhang H-B, Yan Q, Zheng W-G, He Z, Yu Z-Z. Tough Graphene–Polymer Microcellular Foams for Electromagnetic Interference Shielding. ACS Applied Materials & Interfaces. 2011;3(3):918-24.
12. Zhu J, Wei S, Haldolaarachchige N, Young DP, Guo Z. Electromagnetic Field Shielding Polyurethane Nanocomposites Reinforced with Core–Shell Fe–Silica Nanoparticles. The Journal of Physical Chemistry C. 2011;115(31):15304-10.
13. Zhao B, Hamidinejad M, Wang S, Bai P, Che R, Zhang R, et al. Advances in electromagnetic shielding properties of composite foams. Journal of Materials Chemistry A. 2021;9(14):8896-949.
14. Biswas S, Panja SS, Bose S. Tailored distribution of nanoparticles in bi-phasic polymeric blends as emerging materials for suppressing electromagnetic radiation: challenges and prospects. Journal of Materials Chemistry C. 2018;6(13):3120-42.
15. Zhao B, Shao G, Fan B, Zhao W, Xie Y, Zhang R. Synthesis of flower-like CuS hollow microspheres based on nanoflakes self-assembly and their microwave absorption properties. Journal of Materials Chemistry A. 2015;3(19):10345-52.
16. Zhao B, Li Y, Zeng Q, Wang L, Ding J, Zhang R, et al. Galvanic Replacement Reaction Involving Core–Shell Magnetic Chains and Orientation-Tunable Microwave Absorption Properties. Small. 2020;16(40):2003502.
17. Wang G, Zhang D, Wan G, Li B, Zhao G. Glass fiber reinforced PLA composite with enhanced mechanical properties, thermal behavior, and foaming ability. Polymer. 2019;181:121803.
18. Asoodeh F, Aghvami-Panah M, Salimian S, Naeimirad M, khoshnevis H, Zadhoush A. The Effect of Fibers' Length Distribution and Concentration on Rheological and Mechanical Properties of Glass Fiber–Reinforced Polypropylene Composite. Journal of Industrial Textiles. 2021:152808372110432.
19. Aghvami-Panah M, Panahi-Sarmad M, Seraji AA, Jamalpour S, Ghaffarian SR, Park CB. LDPE/MWCNT and LDPE/MWCNT/UHMWPE self-reinforced fiber-composite foams prepared via supercritical CO2: A microstructure-engineering property perspective. The Journal of Supercritical Fluids. 2021;174:105248.
20. Jamalpour S, Ghaffarian SR, Goldansaz H, Jangizehi A. Improving microcellular foamability of amorphous supramolecular polymers via functionalized nanosilica particles. Polymer Composites. 2019;40(1):364-78.
21. Miller D, Kumar V. Microcellular and nanocellular solid-state polyetherimide (PEI) foams using sub-critical carbon dioxide II. Tensile and impact properties. Polymer. 2011;52(13):2910-9.
22. Ameli A, Nofar M, Park CB, Pötschke P, Rizvi G. Polypropylene/carbon nanotube nano/microcellular structures with high dielectric permittivity, low dielectric loss, and low percolation threshold. Carbon. 2014;71:206-17.
23. Wan F, Tran MP, Leblanc C, Béchet E, Plougonven E, Léonard A, et al. Experimental and computational micro-mechanical investigations of compressive properties of polypropylene/multi-walled carbon nanotubes nanocomposite foams. Mechanics of Materials. 2015;91:95-118.